Reports

Obsidian Hydration Profiles Measured by Sputter-Induced Optical Emission

Abstract. *The variation of concentrations of hydrogen, sodium, potassium, lithium, calcium, magnesium, silicon, and aluminum as a function of depth in the hydration layer of obsidian artifacts has been determined by sputter-induced optical emission. The surface hydration is accompanied by dealkalization, and there is a buildup of alkaline earths, calcium and magnesium in the outermost layers. These results have clarified the phenomena underlying the obsidian hydration dating technique.*

When a fresh surface of obsidian is exposed to the atmosphere, the diffusion of ambient water causes a hydrated layer to form on the surface. The measurement of the thickness of this hydrated layer, which varies from less than 1 to over 50 μm depending on the time of exposure, by optical microscopy forms the basis of archeological dating of obsidian artifacts (*1*). Lee *et al.* (*2*) have used a $^{1}H(^{19}F,\alpha\gamma)^{16}O$ resonant nuclear reaction to study the H concentration as a function of depth in obsidians. More recently, Lanford (*3, 4*) has shown that one can date man-made glass objects by measuring the H depth profile in the hydrated layer using the $^{1}H(^{15}N,\alpha\gamma)^{12}C$ nuclear reaction. We report here on the use of sputter-induced optical emission to study the variation in the H concentration and the various constituent elements of obsidian as a function of depth in order to understand the mechanisms of the hydration process. Such an understanding is essential not only to obsidian dating but also to important glass applications such as the encapsulation of radioactive wastes in repositories and the improvement of glass durability.

Characterization of solid surfaces by sputter-induced optical emission has been successfully demonstrated during the past few years (*5*). The principle of the method consists of the detection of optical line spectra emitted by atoms ejected from a solid surface when bombarded by an energetic ion beam. Figure 1 shows a spectral scan of the prominent optical lines of the major and trace elements in an obsidian under ion bombardment with 18-keV Ar^+. A concentration-versus-depth profile of a particular element can be obtained if the intensity of the appropriate spectral line is monitored as a function of sputtering time. Recently, Tsong and Bhalla reported a study of the OH-F exchange in GdF_3 films (*6*) in which the H and F profiles were measured by this method.

The major chemical constituents of obsidian are SiO_2, Al_2O_3, CaO, Na_2O, K_2O, Fe_2O_3, MgO, and TiO_2. Typical concentrations of these components have been given by Ericson *et al.* (*7*). It has been shown by Hench and his coworkers (*8–10*) that silicate glasses hydrate by a process in which alkali metals are leached out by exchange with protons while the silicate network remains more or less intact. A hydronium-alkali ion-exchange reaction of the type

$$Na^+ \text{ (glass)} + 2H_2O \rightarrow H_3O^+ \text{ (glass)} + NaOH$$

has been proposed by Doremus (*11*) and observed experimentally by Lanford (*4*). One can use sputter-induced optical emission to study the exchange process between H and alkali by measuring the depth profiles of H as well as the alkali metals Na, K, and Li and the alkaline earths Ca and Mg. If indeed it can be shown that the hydration layer in obsidian is deficient in alkali ions, then this will provide an alternative and more sensitive method for obsidian dating since the optical emission from the alkalis is generally several orders of magnitude more intense than that for H.

The obsidian samples were bombarded with an Ar^+ ion beam in the energy range 14 to 18 keV. The ion beam unit (supplied by General Ionex Corporation) consisted of a duoplasmatron ion source and a gridded decelerating gap lens. The details of this instrument have been described elsewhere (*12*). The high ion current output from this ion beam system makes it possible for depth-profiling to be done at a very fast rate. A typical current density of 20 $\mu A\ mm^{-2}$ will sputter the obsidian samples at a rate in excess of 10 $\mu m\ hour^{-1}$. At this sputtering rate, depth profiles of even very old obsidian artifacts with thick hydrated surface layers can be obtained within an hour or so. Surface charging was minimized because the sample surface was flooded with electrons from a heated LaB_6 filament positioned near the target holder. A monochromator and a photomultiplier were used for optical detection. The spectral lines selected for depth profiling are as follows: 6563 Å for H, 5890 Å for Na, 7665 Å for K, 6708 Å for Li, 4227 Å for Ca, 2852 Å for Mg, 2882 Å for Si, and 3962 Å for Al.

Figure 2 shows the depth profiles of the various elements in a typical obsidian artifact excavated from Kaminaljuyu, Guatemala (*13*). We calibrated the depth scale by measuring the time taken to sputter through an obsidian film of known thickness deposited on an Al substrate by radio-frequency sputtering. We did this by observing the abrupt drop in the Na signal as the ion beam went through the interface between the obsidian film and the Al substrate. A similar calibration method has been described

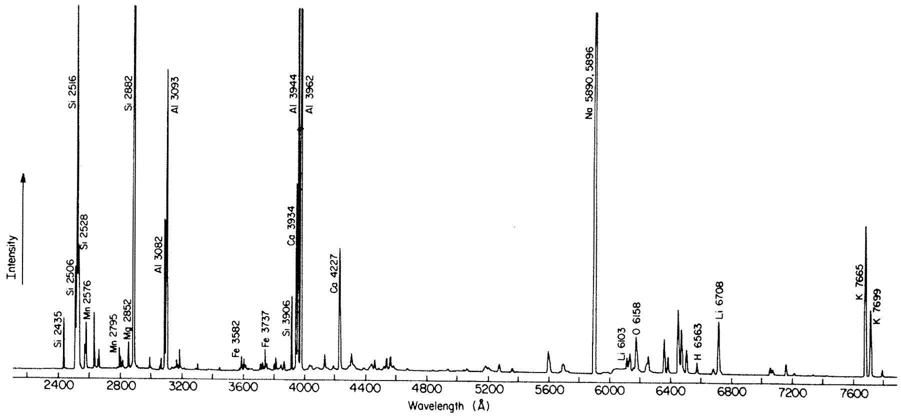

Fig. 1. Spectral scan of the sputter-induced optical emission produced by the bombardment of 18-keV Ar^+ on a rhyolitic obsidian sample.

0036-8075/78/0728-0339$00.50/0

elsewhere (*6*). The accuracy of this calibration is reflected in the agreement between the depth of around 2 μm where the signals of H, Na, K, and Li (Fig. 2, a–d) reach an equilibrium level and the thickness of the hydration band of 2.0 μm measured by the conventional optical microscopy method.

We also measured the depth profiles of the eight elements on freshly cleaved surfaces of the same obsidian artifact. In contrast to the profiles shown in Fig. 2, these optical intensities show no variation as a function of the sputtering time, an indication that hydrated surface layers are absent.

The H profile (Fig. 2a) is similar to those determined by Lee *et al.* (*2*) and Lanford (*3*), using the nuclear reaction technique. The shape of the profile is indicative of a diffusion process where the diffusion coefficient is concentration-dependent (*14*). The initial sharp peak is due to H impurities adsorbed on the sample surface. It is present in nearly all H profiles and has been observed in samples other than obsidians. The H signal gradually approaches an equilibrium value at a depth exceeding 2 μm. If we assume that the equilibrium signal represents the bulk H_2O concentration, which is around 0.3 percent (by weight) (*2, 15*), then the peak H concentration in the hydration layer is only about 1 percent. We believe that the H signal at the equilibrium level should be much lower. The observed high equilibrium signal level is probably due to a contribution from background H contaminants in the Ar^+ ion beam (which was not mass-analyzed) and in the vacuum system (which was at a pressure of 2×10^{-6} torr when the ion beam was in operation).

The depletion of alkali metals in the surface layer is clearly shown in Fig. 2, b–d. The profiles for all three alkalis have approximately the same shape, including Li which is only a minor element in obsidian. However, although Na shows an almost complete depletion in the first few nanometers, that is, the topmost layers, both K and Li have nonzero values in this region. Interestingly, if we extrapolate the sloping part of the profiles to the front edge, the degree of depletion measured as the fraction removed at the surface varies in a regular way with the atomic weight of the alkali: Li, 56 percent; Na, 31 percent; and K, 21 percent. The thickness of the alkali-depleted layer appears to be the same, about 2 μm for all three alkalis. This result seems to suggest that migration into and out of the surface is by a common mechanism.

The depth profiles of Ca and Mg (Fig. 2, e and f) exhibit a somewhat different pattern. The alkaline earths appear to be leached, although the profiles are more irregular and the fraction leached is smaller than for the alkalis. The depth of the depleted layer for both Ca and Mg is close to 2 μm, although it is less clear-cut than for the alkalis. However, most interesting is the apparent pileup of both Ca and Mg in the near-surface layers. A similar Ca peak was observed in the near-surface region of leached soda-lime glass by Clark *et al.* (*10*), using a combination of Auger electron spectroscopy and ion milling. Although the structure of this outermost surface layer is not known, it can be argued that there is

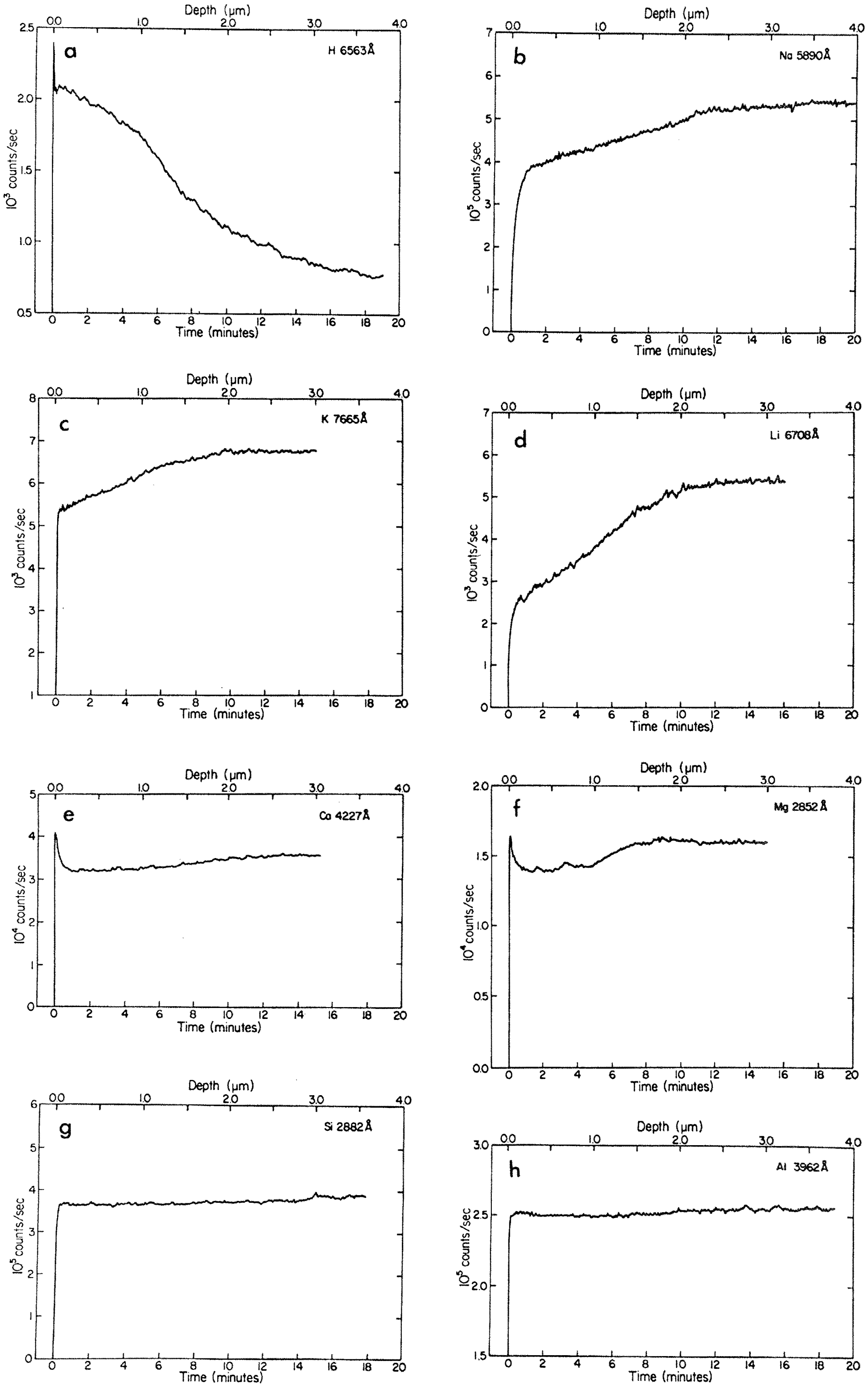

Fig. 2. Depth profiles of (a) hydrogen, (b) sodium, (c) potassium, (d) lithium, (e) calcium, (f) magnesium, (g) silicon, and (h) aluminum in an obsidian artifact from Kaminaljuyu, Guatemala, plotted as the number of photon counts versus the sputtering time and depth. The time constant was 0.3 second; the bombarding conditions consisted of 16-keV Ar^+ with an ion current of 12 μA on a spot 1 mm in diameter.

some reaction between Ca (or Mg) and the alkali-depleted aluminosilicate framework forming perhaps alkaline earth silicates. It has been suggested that a silicate layer of this kind can act as a diffusion barrier (*10*) and as such may disrupt the regular growth of the hydration layer which is the basis of the obsidian dating technique.

The Si and Al depth profiles (Fig. 2, g and h) show very little variation of concentration with depth, indicating no replacement of Si or Al by H as expected. The depletion of the major alkalis and part of the alkaline earths means that there is an increase in the mole fraction of SiO_2 and Al_2O_3 at the surface. The essentially constant signal from these elements suggests that the densities of Si and Al remain constant. This result supports the idea that the aluminosilicate framework remains intact during leaching under near-neutral conditions. Hench (*8*) has reasoned from his glass-leaching studies that the formation of a silica-rich and alumina-rich surface layer acts as a protective film to further leaching. Hench and Clark (*9*) have reported that the thickness of the silica-rich or alkali-depleted layer is controlled by a $t^{1/2}$ dependence, which changes to a t dependence as the leaching time, t, increases. Despite the different hydration conditions, it is possible that obsidian may hydrate in a similar manner, as has been suggested by the results of Ericson *et al.* (*7*).

The results of this investigation demonstrate that the thickness of the hydration layer on obsidian artifacts can be established by the technique of sputter-induced optical emission. The depth profiles of the different elements suggest that the kinetics of diffusion in obsidian are highly complex and that chemical composition plays an important role in the hydration process (*1*, *16*). This technique not only provides a new method for obsidian dating but can also be applied to the study of other pertinent problems such as the hydration of container glass surfaces by aqueous solutions and the leaching of proposed glasses for the encapsulation of radioactive wastes.

I. S. T. TSONG
C. A. HOUSER
N. A. YUSEF, R. F. MESSIER
W. B. WHITE
Materials Research Laboratory,
Pennsylvania State University,
University Park 16802
J. W. MICHELS
Department of Anthropology,
Pennsylvania State University

References and Notes

→ I. Friedman and R. L. Smith, *Am. Antiq.* **25**, 476 (1960).
2. R. R. Lee, D. A. Leich, T. A. Tombrello, J. E. Ericson, I. Friedman, *Nature (London)* **250**, 44 (1974).
3. W. A. Lanford, *Science* **196**, 975 (1977).
4. ———, *Nucl. Instrum. Methods* **149**, 1 (1978).
5. N. H. Tolk, I. S. T. Tsong, C. W. White, *Anal. Chem.* **49**, 16A (1977); I. S. T. Tsong and A. C. McLaren, *Spectrochim. Acta Part B* **30**, 343 (1975); C. W. White, D. L. Simms, N. H. Tolk, *Science* **177**, 481 (1972).
6. I. S. T. Tsong and A. S. Bhalla, *Appl. Phys. Lett.* **32**, 381 (1978).
7. J. E. Ericson, A. Makishima, J. D. Mackenzie, R. Berger, *J. Non-Cryst. Solids* **17**, 129 (1975).
8. L. L. Hench, in *Ceramics and Glass Radioactive Waste Forms Workshop* (Report CONF-770102, Energy Research and Development Administration, Washington, D.C., 1977), p. 189.
9. L. L. Hench and D. E. Clark, *J. Non-Cryst. Solids* **28**, 83 (1978).
10. D. E. Clark, M. F. Dilmore, E. C. Ethridge, L. L. Hench, *J. Am. Ceram. Soc.* **59**, 62 (1976).
11. R. H. Doremus, *J. Non-Cryst. Solids* **19**, 137 (1975).
12. I. S. T. Tsong and R. B. Liebert, *Nucl. Instrum. Methods* **149**, 523 (1978).
13. Sample KJ70-13674 (51-8362) in the collection of the Department of Anthropology, Pennsylvania State University.
14. W. Haller, *Phys. Chem. Glasses* **4**, 217 (1963).
15. J. W. Michels, *Science* **158**, 211 (1967).
→ I. Friedman and W. Long, *ibid.* **191**, 347 (1976).
17. This work was supported in part by the Energy Research and Development Administration under contract EY-76-S-02-2754.

9 February 1978; revised 25 April 1978

Visual Phenomena Induced by Relativistic Carbon Ions With and Without Cerenkov Radiation

Abstract. *Exposing the human eye to individual carbon ions ($^6C^+$) moving at relativistic speeds results in visual phenomena that include point flashes, streaks, and larger diffuse flashes. The diffuse flashes have previously been observed by astronauts in space but not in laboratory experiments with particles of high atomic number and energy. They are observed only when the nucleus moves fast enough to generate Cerenkov radiation.*

There have been a number of investigations designed to determine the physical mechanism behind the visual phenomena observed by astronauts when exposed to the radiation environment in space (*1-5*). Our earlier experiments with muons, pions, and individual nitrogen nuclei (*3*) showed that Cerenkov radiation generated within the eye can induce visual phenomena similar in description to those reported by astronauts in deep space (*1*). However, the muon and pion data were obtained in experiments designed to simulate the passage of an ion of high atomic number, Z, and energy, E, with a pulse containing $N = Z^2$ singly charged particles. This raised the question of the extent to which the phenomena observed resembled those induced by the HZE (high Z and E) particles encountered in space (*6*). Moreover, experiments with neutrons, alpha particles, and nitrogen nuclei (*5*) showed that star- and streak-like phenomena similar to some of those observed in space can be induced in the absence of Cerenkov radiation, presumably as the result of ionizations and excitations along the trajectory of the incident particle or its secondaries. This raised the possibility that the HZE particles that generated visible pulses of Cerenkov light in the eyes of astronauts on Apollo missions would have been detected anyway because of ionization effects, and that while Cerenkov radiation may have influenced the visual phenomena experienced, it would not have significantly affected the rate at which the flashes were observed.

To directly compare the visual phenomena induced by HZE particles with and without Cerenkov radiation and to determine the effect of Cerenkov radiation on a subject's ability to detect the particles, we initiated a series of exposures of human subjects to HZE particles at the Bevalac accelerator at Lawrence Berkeley Laboratory. The details of the facility devised to deliver HZE particles one at a time are given elsewhere (*7*). This report describes the results of the preliminary trials, which involved comparing carbon nuclei at speeds above and below the Cerenkov threshold. The nuclei had kinetic energies of 595 MeV per nucleon and a stopping power in water of 94 MeV-cm^2/g at the higher speed, and values of 470 MeV per nucleon and 103 MeV-cm^2/g at the lower speed. The carbon nuclei do not stop in the eye, nor do they lose a significant amount of energy in traversing it. The patterns of ionizations and excitations along the trajectories are quite similar for the two cases, and a significant increase in a subject's ability to detect the passage of a higher-velocity nucleus through his eye would be attributable to Cerenkov radiation.

After dark-adapting for 40 minutes, the subject aligned himself to the beam line by using a personalized bite plate and fixated on a red light-emitting diode mounted on the far wall of the darkened room. This aligned the head and eye